Gyroid Structures for Use in Implants, their Characteristics and Mesh Generation

L. Řehounek[1,*], A. Jíra[1], J. Vorel[1]

[1] *Czech Technical University in Prague, Faculty of Civil Engineering, Thákurova 7, 166 29 Prague 6, Czech Republic*

[*] *lubos.rehounek@fsv.cvut.cz*

Abstract: This contribution presents the results of a study on gyroid structures for use in implants. The recent advent of additive manufacturing technologies enables rapid prototyping of specimens and experimental design of novel structures to achieve osseointegration. Sample gyroid structure specimens were 3D-printed via selective laser sintering (SLS) using the PA-12 polymer powder and uniaxially tested for peak stress and global elastic modulus. A great benefit is the shapeability of the structure and its predictability by FEM. Generation of this structure can either be done via CAD environments or direct modelling with the gyroid equation. Finite element method (FEM) simulations confirm the values of Young's moduli between the experiment and simulation are within ca. 15 % conformity. This approach will enable more custom designs in the future without the need for testing of every variant.

Keywords: gyroid; porous; FEM; 3D printing; osseointegration.

1 Introduction

Removal of typical stress from the bone by introducing a stiff metal implant often leads to reduction of bone mass in the adjacent bone [1]. The typical values of Young's modulus E for human bone is ca. 17.1±3.5 GPa [2] as opposed to ca. 100–120 GPa for titanium and its alloys. One of the main driving forces of novel design in the field of implantology is the motion to decrease the number of revision surgeries and reduce the risk of aseptic loosening of the implant [3]. The principal means of achieving good osseointegration of implants are usually various forms of surface treatment to increase the surface roughness (and therefore the contact area of bone) or manipulate the chemical properties of the surface [4]. Among those, the most notable are [5]:

- Blasting with particles
- Chemical etching
- Plasma-sprayed surfaces
- Ion-sputtering coating
- Anodized surface
- HA coating
- Porous surfaces

The approach to apply a porous surface stems from the need to increase the surface area at the bone-implant interface and also provide a localized area where bone trabeculae can grow *inside* the body of the implant itself. The gyroid structure has the potential to create a bone-implant composite material that can reduce (or eliminate) the effects of stress shielding [6] and create a continuous gradient of material properties in the radial implant-bone directions. The fact that bone trabeculae can effectively grow inside the implant and create an interconnected mechanism has been investigated in one of the authors' previous works [7] in in vivo tests on laboratory pigs with use of a different porous structure.

2 Gyroid equation modelling

The modelling of the structure can be done in two ways; either via CAD or directly with equations. We found that with all 3D printing applications, the former approach is usable and models have good quality for

metal or plastic SLS printing. However, when FEM is considered, this approach falls short on precision as the surface mesh is intersecting and tesselation quality is bad (Fig. 1), preventing the enclosure of a solid. Rather, modelling with the TPMS (triply-periodic minimal surface) single gyroid equation (Eq. (1) can be adopted:

$$\sin\left(\frac{2\pi x}{a}\right)\cos\left(\frac{2\pi y}{a}\right)+\sin(\frac{2\pi y}{a})\cos\left(\frac{2\pi z}{a}\right)+\sin\left(\frac{2\pi z}{a}\right)\cos\left(\frac{2\pi x}{a}\right)-t=0, \tag{1}$$

where a represents the length of a circumsribed cube and x, y and z are spatial coordinates. The parameter t influences the curvature of the gyroid structure and by its manipulation we can transfer between the *sheet* and *tubular* variants of the structure.

Following the creation of the TPMS gyroid, a volumetric gyroid structure can be created by intersecting the generated surfaces with a homogeneous body (either the sheet or the tubular phase of the gyroid).

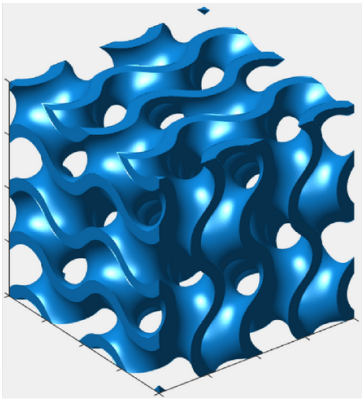

(a) Sample sheet-based single gyroid structure

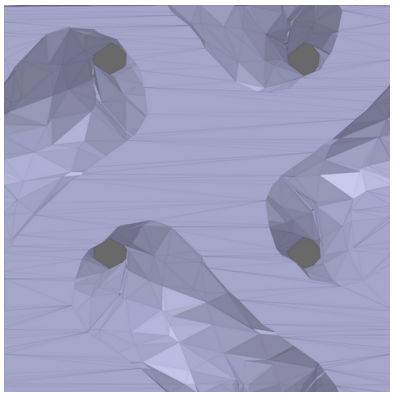

(b) CAD-generated with bad tesselation

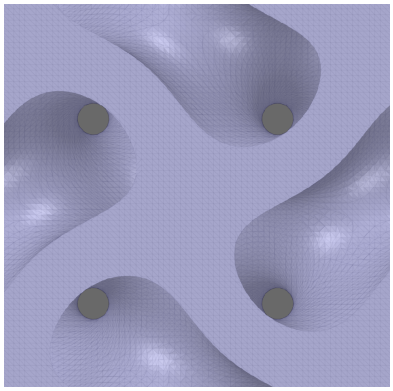

(c) Directly generated with good tesselation

Fig. 1: A typical sheet gyroid structure and details of individual means of generation with corresponding quality of tesselation. The cutouts (b) shows various errors such as overlapping faces and out-of-boundary vertices; while usually suitable for 3D printing, this generation is unaccetable for numerical analyses. Generated with MSLattice [8].

3 Mechanical tests and FEM simulations

To verify the reliability of FEM numerical analyses and compare the various variants of porous structures in regard to their mechanical properties, we performed uniaxial compression tests on sample gyroid structure specimens with relative theoretical density of $n = 0.75$ (corresponding value $t = 0.39$ for the sheet gyroid variant and $t = 0.78$ for the tubular gyroid, see Eq. (1). These specimens had dimensions of $25.12 \times 25.12 \times 25.12$ mm and had two homogeneous load-distributing plates fitted on the top and bottom. The test was carried out in the mode or controlled displacement of 1 mm/min using the electromechanic MTS Alliance RT30kN and RT50kN loading machines. The specimens were made and subsequently processed using the PA-12 polymer material on the Sinterit Lisa Pro 3D printer. Also, one Dode-Thick trabecular specimen with the same parameter of porosity was included. The uniaxial compression tests were controlled by constant velocity of displacement. The specimens are shown on Fig. 2. The test was carried out to determine the values of *global* Young's moduli E of whole individual structures in regard to comparison of viability of various geometrical variants with the same porosity under the same conditions.

4 Results and conclusions

The results of uniaxial compression tests are shown together with the results of X-FEM simulations using a strain-based periodic numerical homogenization method in Tab. 1. The proposed homogenization method was performed in a Matlab-based software the reader can learn more about in [10]. As expected, the sheet gyroid variant shows the most stiff response combined with a less localized damage behavior (Fig. 3), which

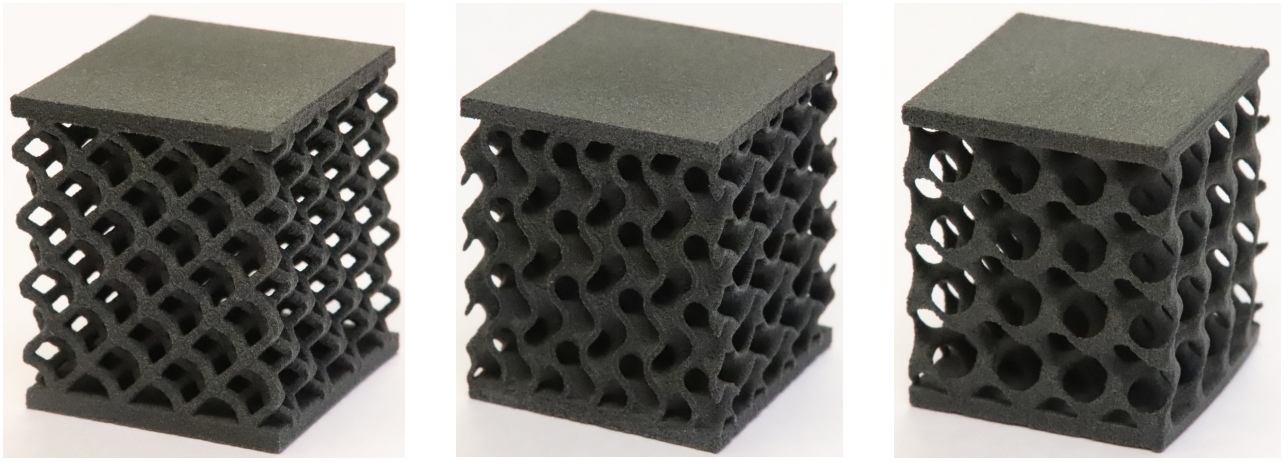

(a) Dode-Thick trabecular (b) Single sheet gyroid (c) Tubular single gyroid

Fig. 2: Three PA-12 3D-printed specimens for uniaxial compressive tests. The variants all have the same porosity $n = 0.75$.

is beneficial to implant-oriented applications as the risk of chipping and wear debris polluting the surrounding tissue of the patient is a concern for osteolysis [9].

Tab. 1: The results of uniaxial compression tests and numerical analyses (X-FEM) of the porous structures in regard to the *global* Young's modulus.

Structure variant	Compression test E [MPa]	X-FEM Homogenization E [MPa]
Dode-Thick	27.3 ± 3.8	26.4
Sheet gyroid	28.7 ± 1.8	33.2
Tubular gyroid	72.4 ± 6.1	82.9

(a) Dode-Thick trabecular (b) Single sheet gyroid (c) Tubular single gyroid

Fig. 3: All destroyed specimens after failure caused by the uniaxial compression test. Note the total dislocation and shear character of failure of (a) and (c) compared to the sheet gyroid variant (b).

Porous structures offer a solution to increasing the surface area of an implant, their system of interconnected pores allows for good fluid transport and the sheet character of their geometry does not allow for a local failure. Therefore, it seems to be worthwhile to explore the gyroid variants (single, double) in regard to optimal geometry for implant applications. Experience showed us that CAD generation is not a viable approach as the tesselation quality is bad. With direct modelling, we can achieve a good quality mesh for the purpose of

optimizing the geometry via FEM analyses; mainly in regard to matching the global Young's modulus E of the structure to human bone. To further the understanding of the topic, the authors plan to launch experiments on metal SLS 3D-printed specimens to determine values of E in regard to the porosity and other geometrical parameters of the structure with the final goal of implementing it onto a surface of a functional implant, moving from polymer SLS into the area of fully SLS 3D-printed metal implants with surface porous structures.

The design should always include requirements from both mechanical and biological standpoints as strictly matching the elastic modulus of bone might not always be the first priority. While porous structures lend themselves to design of structures with much lower global moduli E (benefitial for prevention of stress-shielding), strength and prevention of localized falure can potentially take precedence in design. If experiments show good quantity of bone ingrowth and an interlocking mechanism with a gradient of material properties is achieved, many other factors such as pore size for optimal bone ingrowth and fluid transport must be considered.

Acknowledgement

The authors would gratefully like to acknowledge the financial support provided by the Faculty of Civil Engineering, CTU, Prague, project n. SGS20/155/OHK1/3T/11.

References

[1] J.E. Bidaux, Metal injection moulding of low modulus Ti–Nb alloys for biomedical applications, Powder Metall 56 (2013) 263–266, doi: 10.1179/0032589913Z.000000000118.

[2] D.T. Reilly, A.H. Burstein, V.H. Frankel, The elastic modulus for bone, Acta Polytech. J. Biomech. 7 (1974) 271–275.

[3] L. Řehounek, F. Denk, A. Jíra, Geometrical optimization of dental implants with regard to osseointegration, Acta Polytech. CTU Proc. 13 (2017) 97–101, doi: 10.14311/APP.2017.13.0097.

[4] J.C. Chen, et al., In vivo studies of titanium implant surface treatment by sandblasted, acid-etched and further anchored with ceramic of tetracalcium phosphate on osseointegration, J Aust Ceram Soc 55 (2019) 799–806, doi: 10.1007/s41779-018-00292-5.

[5] A. Gupta, M. Dhanraj, G. Sivagami, Status of surface treatment in endosseous implant: A literary overview, Indian J Dent Res 21 (2010) 433–438, doi: 10.4103/0970-9290.70805.

[6] R. Ummethala ,et al., Selective laser melting of high-strength, low-modulus Ti–35Nb–7Zr–5Ta alloy, Materialia 14 (2020) p.100941, doi: 10.1016/j.mtla.2020.100941.

[7] L. Řehounek, A. Jíra, Experimental and numerical anylses of a 3D-printed titanium trabecular dental implant, Acta Polytech. 57 (2017) 218–228, doi: 10.14311/AP.2017.57.0218.

[8] O. Al-Ketan, R.K. Abu Al-Rub, MSLattice: A free software for generating uniform and graded lattices based on triply periodic minimal surfaces, MDPC (2020) p.e205, doi: 10.1002/mdp2.205.

[9] H.C. Amstutz, et al., Mechanism and clinical significance of wear debris-induced osteolysis, Clin. Orthop. Relat. Res. (1992) 7–18.

[10] A. Jíra, et al., Mechanical Properties of Porous Structures for Dental Implants: Experimental Study and Computational Homogenization. Materials, 14(16) (2021), p.4592, doi: 10.3390/ma14164592.